Inclusion of a turbulence parameterisation in a diagnostic mass consistent model driven by a prognostic model

S. Trini Castelli, D. Anfossi and G. Belfiore

Institute of Atmospheric Sciences and Climate, National Research Council
ISAC – C.N.R.
Torino, Italy

ISAC-TO RMS modelling system

for air quality and environmental impact assessment

RAMS

Atmospheric circulation model (Regional Atmospheric Modeling System Pielke et al., 1992)

Fields of WIND, TEMPERATURE, T.K.E., K (3 D)
TOPOGRAPHY, SURFACE FLUXES (2 D)

MIRS

MINERVE!

Boundary layer parameterisation interfacing code (Method for Interfacing RAMS and SPRAY Trini Castelli and Anfossi, 1997, Trini Castelli, 2000)

Fields of WIND, K, SKEWNESS/KURTOSIS, σ & T_L (3 D)
TOPOGRAPHY, PBL height (2 D)

SPRAY

Lagrangian-particle dispersion model (Brusasca et al., 1989, Anfossi et al., 1998, Tinarelli et al. 2000, Ferrero et al. 2001)

Fields of PARTICLE POSITIONS
G. L. CONCENTRATION

RAMS-MIRS configuration

Example of a typical configuration for a simulation of the meteo fields using the prognostic code RAMS up to 1 km resolution, 4 nested domains

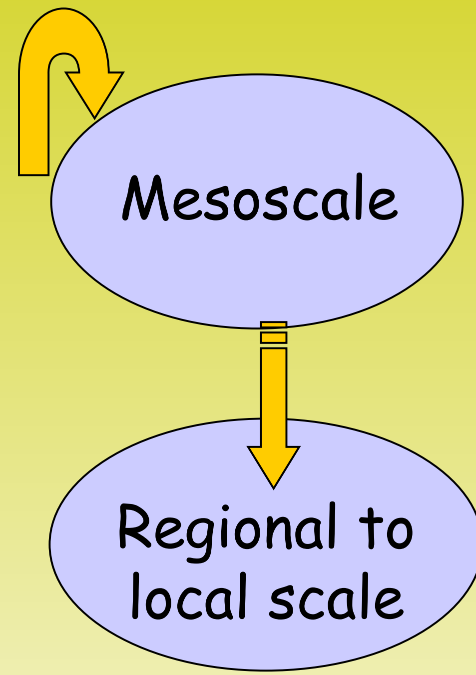

grid 1: 64 km horizontal resolution
grid 2: 16 km horizontal resolution
grid 3: 4 km horizontal resolution
grid 4: 1 km horizontal resolution

Vertical grid: vertical stretched layers, 0 –15/20000 m, *first layer 50 m depth (first level at ~25 m)*

RAMS is initialised with the ECMWF (0.5° lat/lon) analysis fields.

Nudging at the lateral boundaries of the outer grid every 6 hours.

Downscaling from RMS to MINERVE

mass consistent model

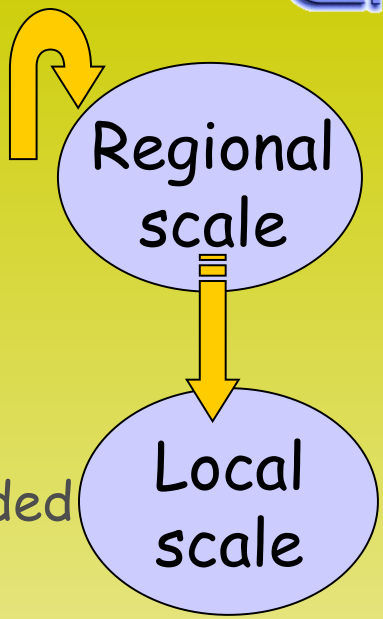

Simulation of the meteo fields using the diagnostic code MINERVE up to ~ 100 m resolution, in subdomains typically 10-20 km x 10-20 km size

MINERVE gets as input the hourly RAMS 3D gridded dynamical and thermal fields and…

- interpolates the mean input fields on its 3D computational domain
-performs and objective analysis: application of mass conservation in every domain cell

Advantages of RAMS→MINERVE downscaling:

-possibility of including local measurements
-possibility of including more detailed topograhy data

An example of how RAMS_MIRS + MINERVE works for wind field in complex terrain *from ALPNAP Alpine Space Project*

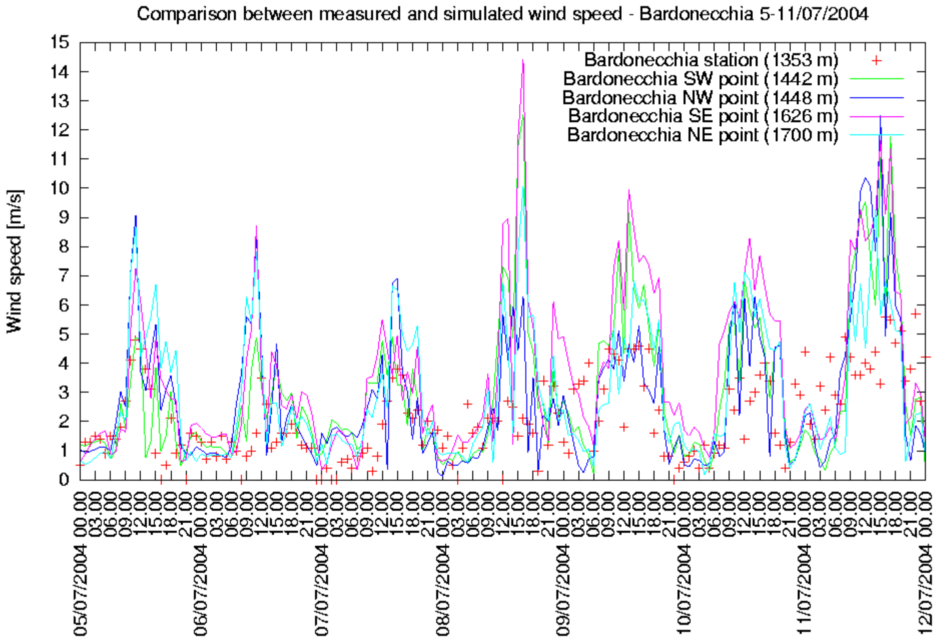

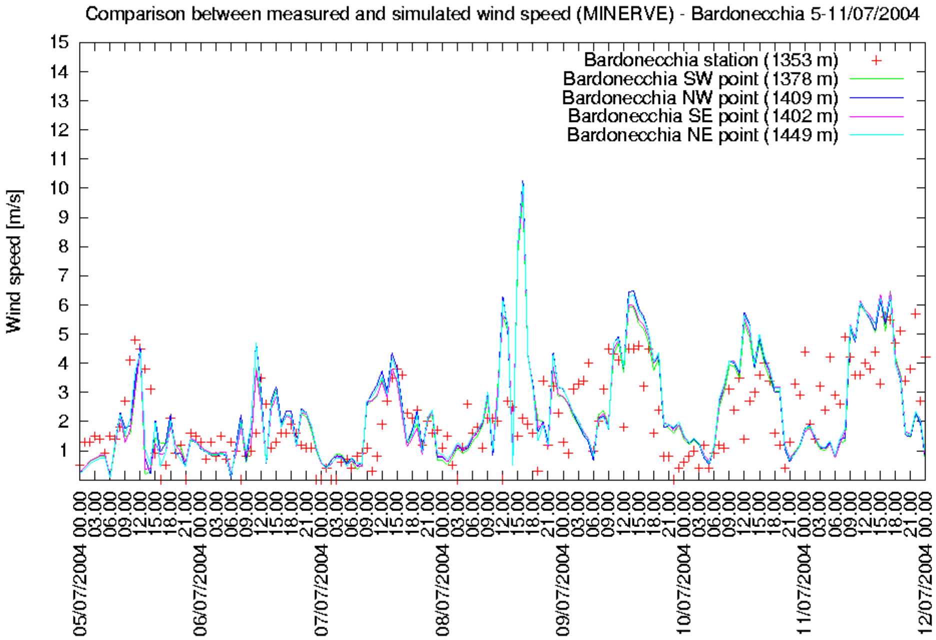

RAMS ----------------> MINERVE

What is this work about

For its nature, MINERVE is not designed to account for the prognostic turbulence fields, and the Lagrangian turbulent variables are thus calculated in SPRAY from parameterisations defined for flat terrain (ex. Hanna, 1982).

In this work we investigate whether a proper interpolation from the coarser-resolution prognostic 3D-gridded turbulence fields, like diffusion coefficients, turbulent kinetic energy and its dissipation, might be used in complex and inhomogeneous terrain.

In this way, the shortcoming of using parameterised turbulent fields might be overcome by coupling MINERVE with a module, which calculates the turbulence fields on the high-resolution diagnostic grid by interpolating from the coarser prognostic grid.

What we compare here

RAMS is run with four nested grids, where the third (G3) and the fourth (G4) grids have respectively 1 km and 250 m resolution.

RAMS fields on **G4** at 250 m are considered the 'truth' versus which to test other two combinations.

The G3 turbulence fields from the 1-km grid are bilinearly interpolated on the 250-m mesh points, originating the turbulence dataset **G3_INTP** to be checked as an alternative to flat-terrain parameterisations.

A downscaling of the mean flow to 250 m with MINERVE, using in input the 1-km resolution grid RAMS G3 fields, is done. MINERVE wind fields at 250 m are then used to calculate the surface layer and boundary layer parameters entering the turbulence calculation in the standard configuration, that is applying the **Hanna (1982)** parameterisation

We consider three different turbulence closure schemes in RAMS……

The *MY 2.5* scheme (as in RAMS)

Vertical diffusion coefficients from the TKE equation in *boundary layer approximation*:

$$\frac{dE}{dt} = \frac{\partial}{\partial z} K_E \frac{\partial E}{\partial z} + P - \varepsilon \qquad \text{with} \qquad K_E = S_E l (2E)^{1/2}$$

$$K_m = S_m l (2E)^{1/2} \qquad \varepsilon = \frac{(2E)^{3/2}}{\Lambda_1} \qquad l = \frac{kz}{1 + kz/l_\infty} \qquad l_\infty = a_\infty \frac{\int z\sqrt{E}\,dz}{\int \sqrt{E}\,dz}$$

S_m, S_E are functions depending on the set of empirical constants (A_1, B_1, A_2, B_2, C) = (0.92, 16.6, 0.74, 10.1, 0.08) and on the shear and buoyancy terms (ref. to Mellor and Yamada (1974,1982)).

Closure length scales: $(l_1, \Lambda_1, l_2, \Lambda_2) = (A_1, B_1, A_2, B_2) l$

Horizontal diffusion coefficients from the deformation scheme as in El-anis…

$$K_{m-horiz} = \rho_0 \max\left[K_{min-h}, (C_x \Delta x)^2 \left\{S_2^{0.5}\right\}\right] \qquad \text{with} \qquad K_{min-h} = 0.075 K_A \left(\Delta x^{4/3}\right)$$

The turbulence closures used in RAMS_MIRS

The EL_(iso)anis scheme

Vertical diffusion coefficients from the 3D TKE (E) equation:

$$\frac{dE}{dt} = \frac{\partial}{\partial x_j} K_E \frac{\partial E}{\partial x_j} + P - \varepsilon \qquad \text{with} \qquad K_E = \alpha_E K_m$$

$$K_m = c_\mu E^{1/2} l \qquad \varepsilon = \frac{c_\varepsilon E^{3/2}}{l_d} \qquad l_d = l = \frac{kz}{1 + kz/l_\infty} \qquad l_\infty = a_\infty \frac{\int z\sqrt{E}dz}{\int \sqrt{E}dz}$$

$c_\mu \quad c_\varepsilon \quad \alpha_E$ *empirical coefficients*

Horizontal diffusion coefficients from a deformation scheme

$$K_{m-horiz} = \rho_0 \max\left[K_{min-h}, (C_x \Delta x)^2 \left\{S_2^{0.5}\right\}\right] \qquad \text{with} \qquad K_{min-h} = 0.075 K_A \left(\Delta x^{4/3}\right)$$

ρ_0 air density, C_x dimensionless coefficient, Δx grid spacing

S_2 horizontal strain rate, K_A user-specified coefficient of order 1.

The case considered

North-West Italian Alpine region around Torino

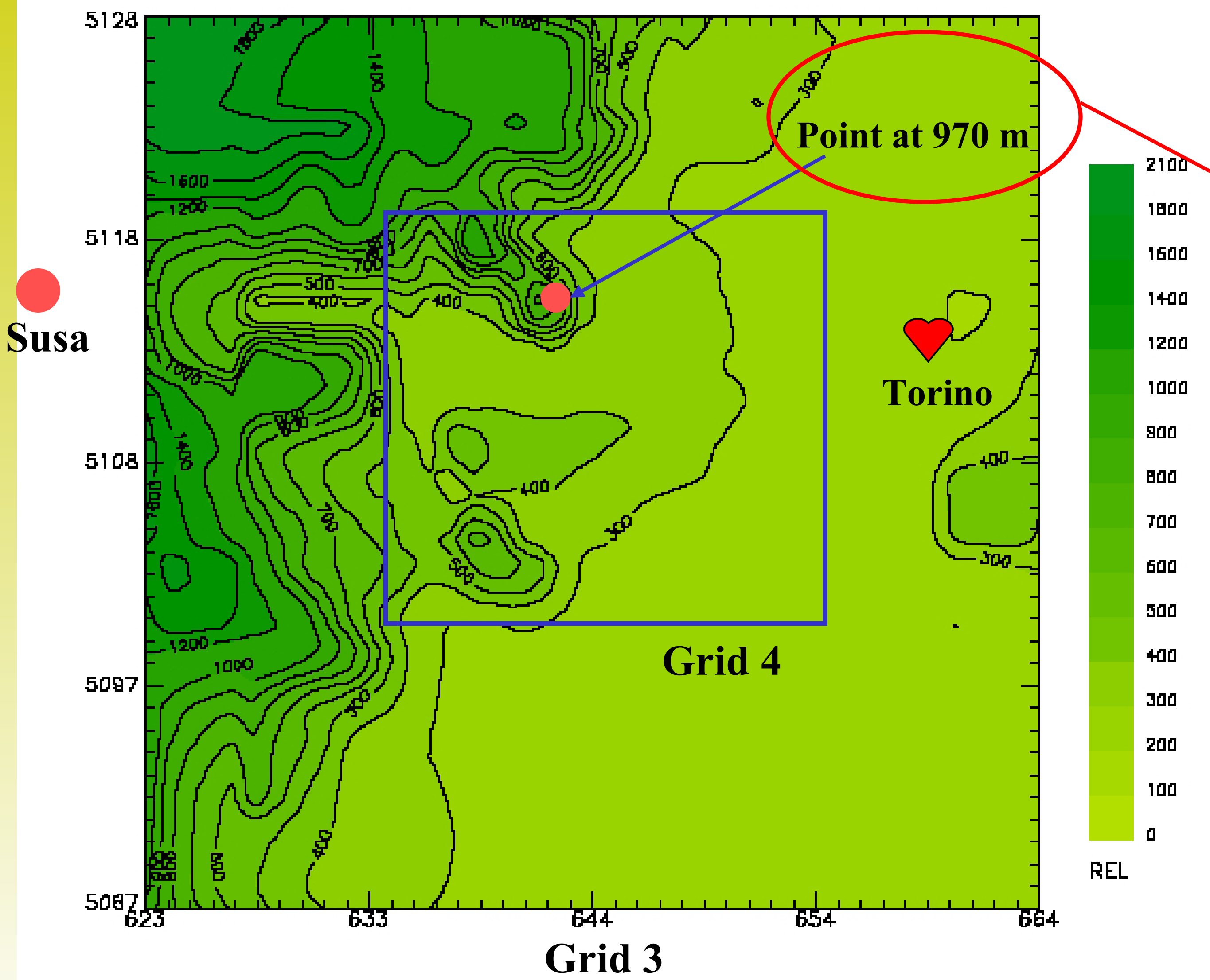

Altitudes……

G4 970 m

G3, 4 points:

NW 772 m
NE 598 m
SE 780 m
SW 939 m

dedicated to COST732 Colleagues…….

The case considered

North-West Italian Alpine region around Torino

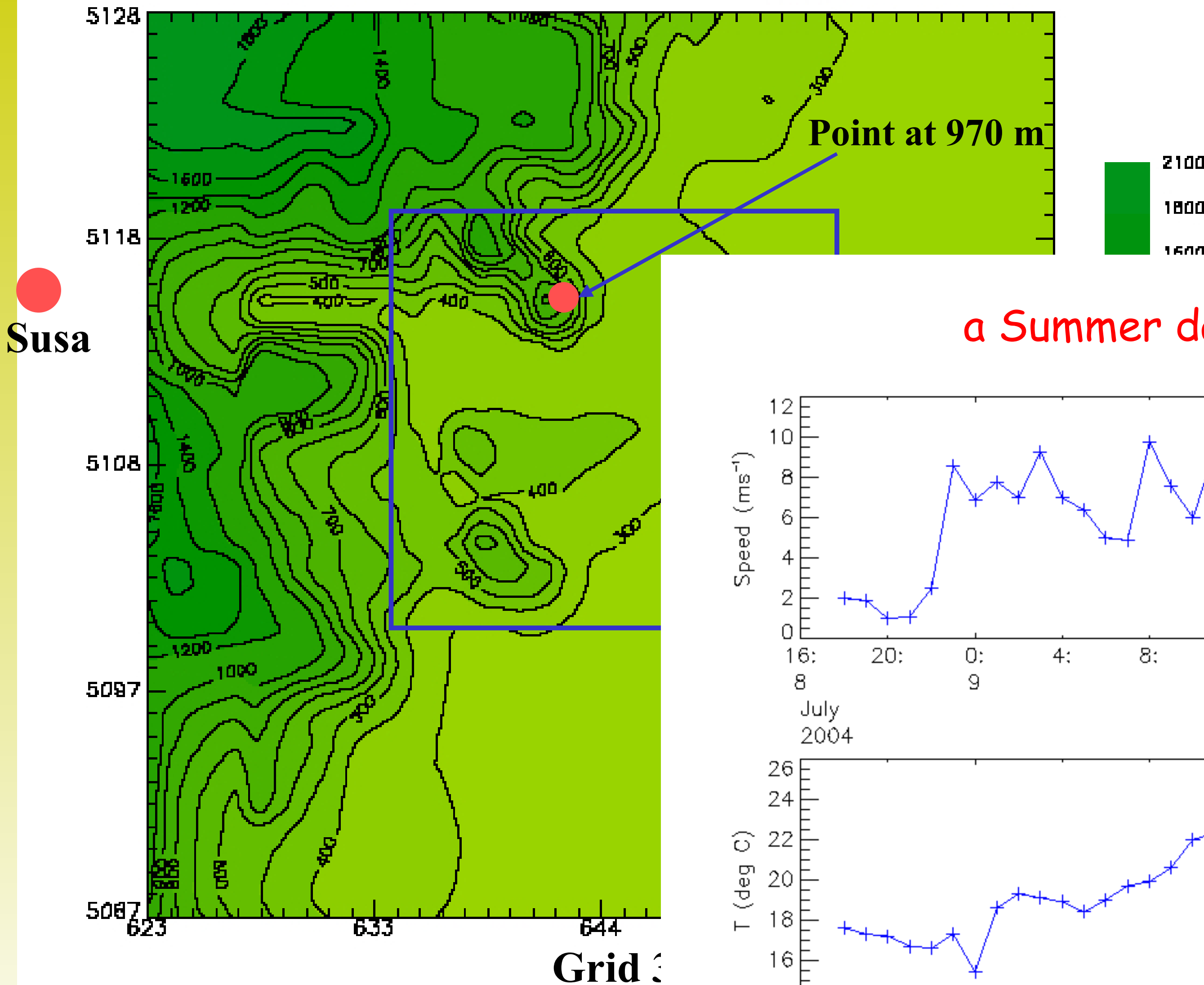

a Summer day, 9 July 2004, in Susa

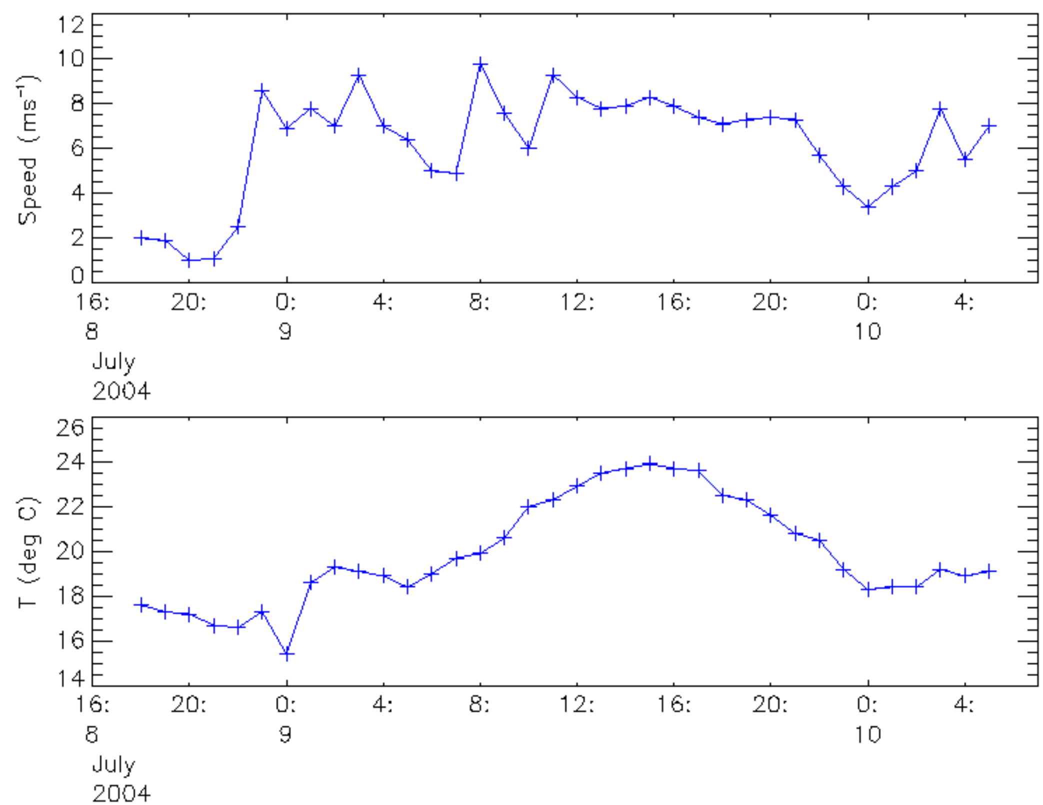

Distributions of TKE for G3_INTP and G4 values (h < 1450 m)

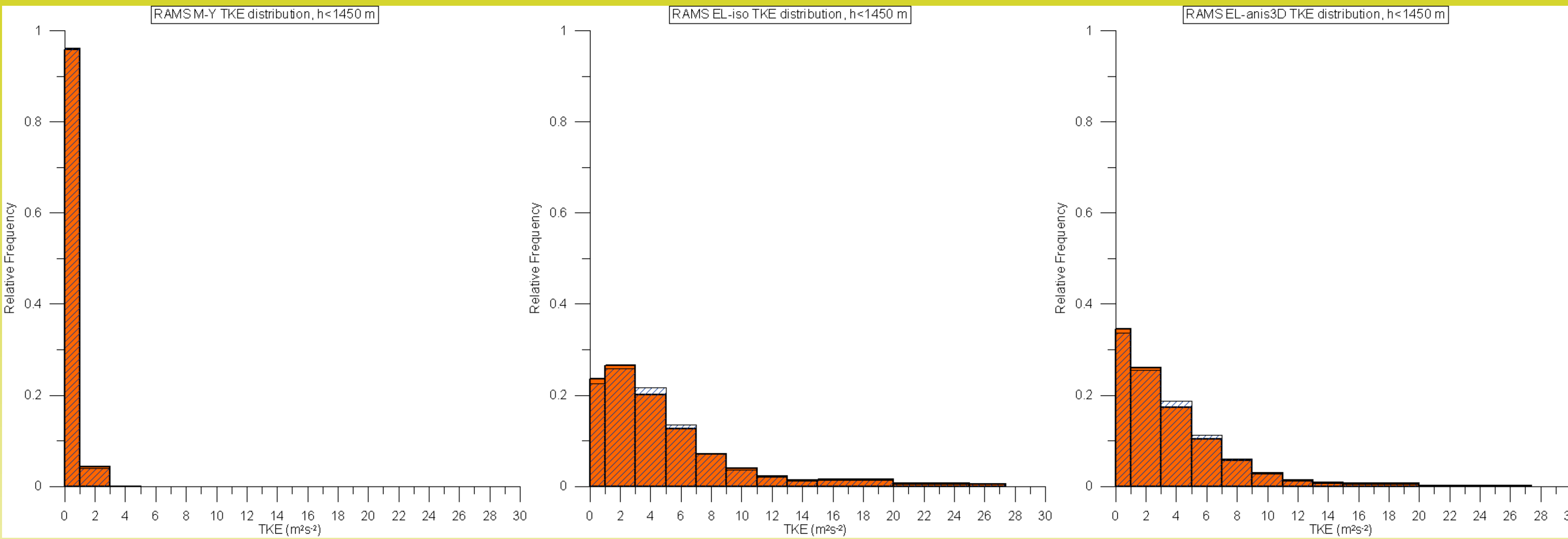

MY2.5 EL_iso EL_anis

Dashed blue: values interpolated from Grid 3
Solid orange: values calculated on Grid 4

Scatter diagrams of G3_INTP TKE vs. G4 TKE values (h < 1450 m)

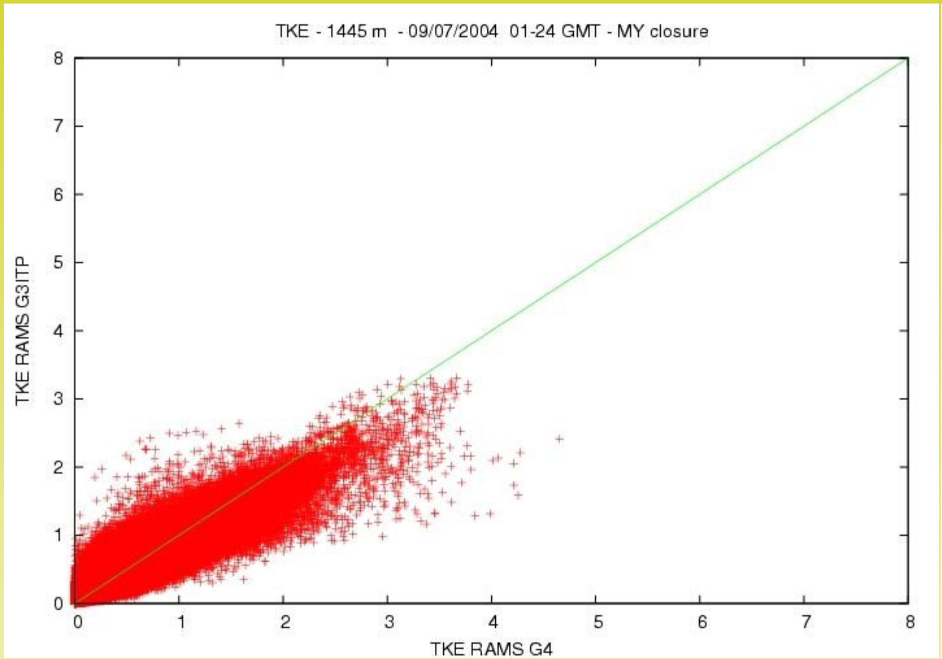

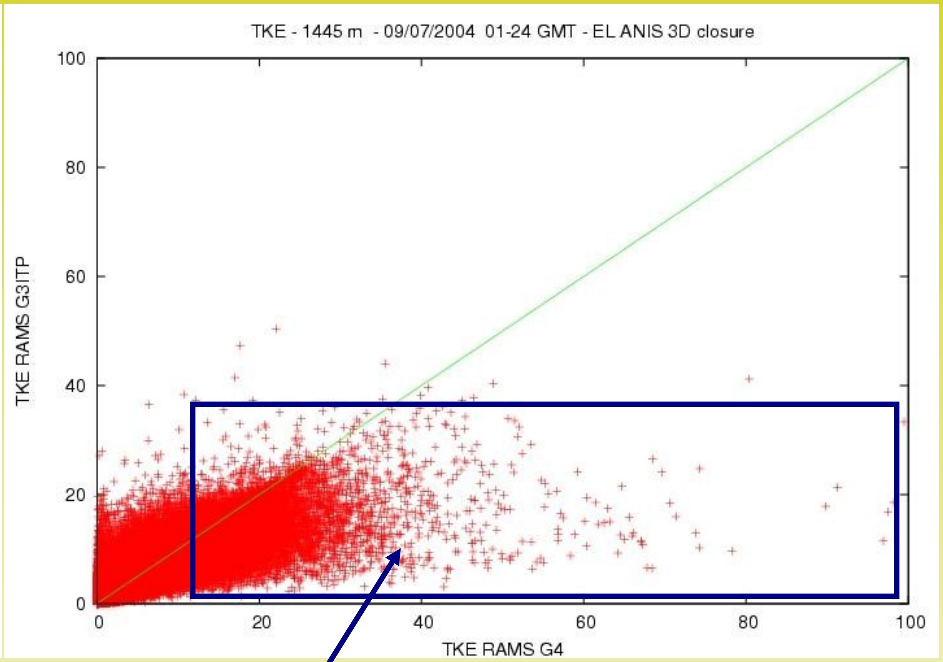

MY2.5

EL_anis

TKE > 10 m^2s^{-2} is ~2% of full dataset (3.172.416)

TKE > 20 m^2s^{-2} is ~0.15 % of full dataset

Time trend of TKE for G3_INTP and G4 values at three model levels - MY 2.5 scheme

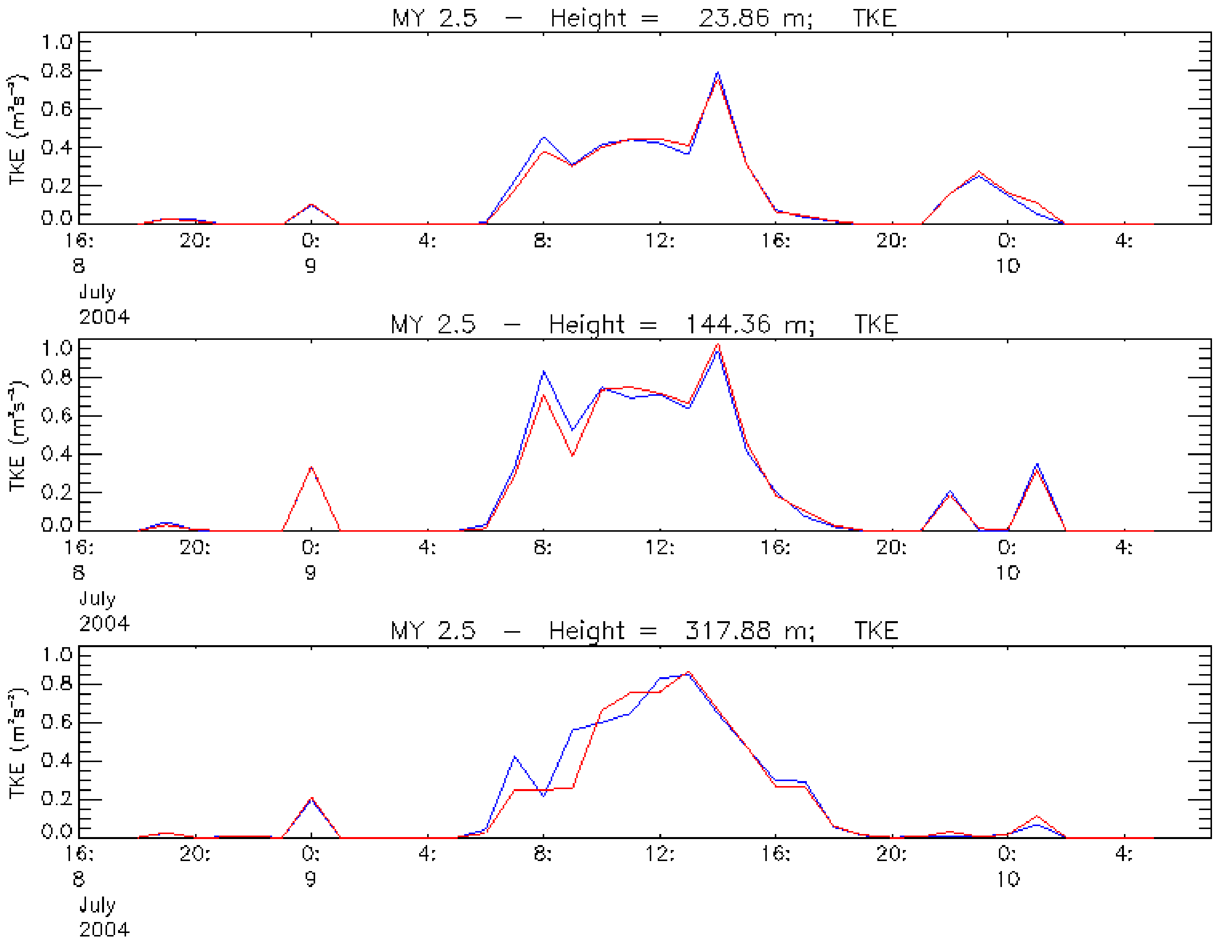

Red: G3_INTP TKE values
Blue: G4 TKE values

Time trend of TKE for G3_INTP and G4 values at three model levels - EL_iso scheme

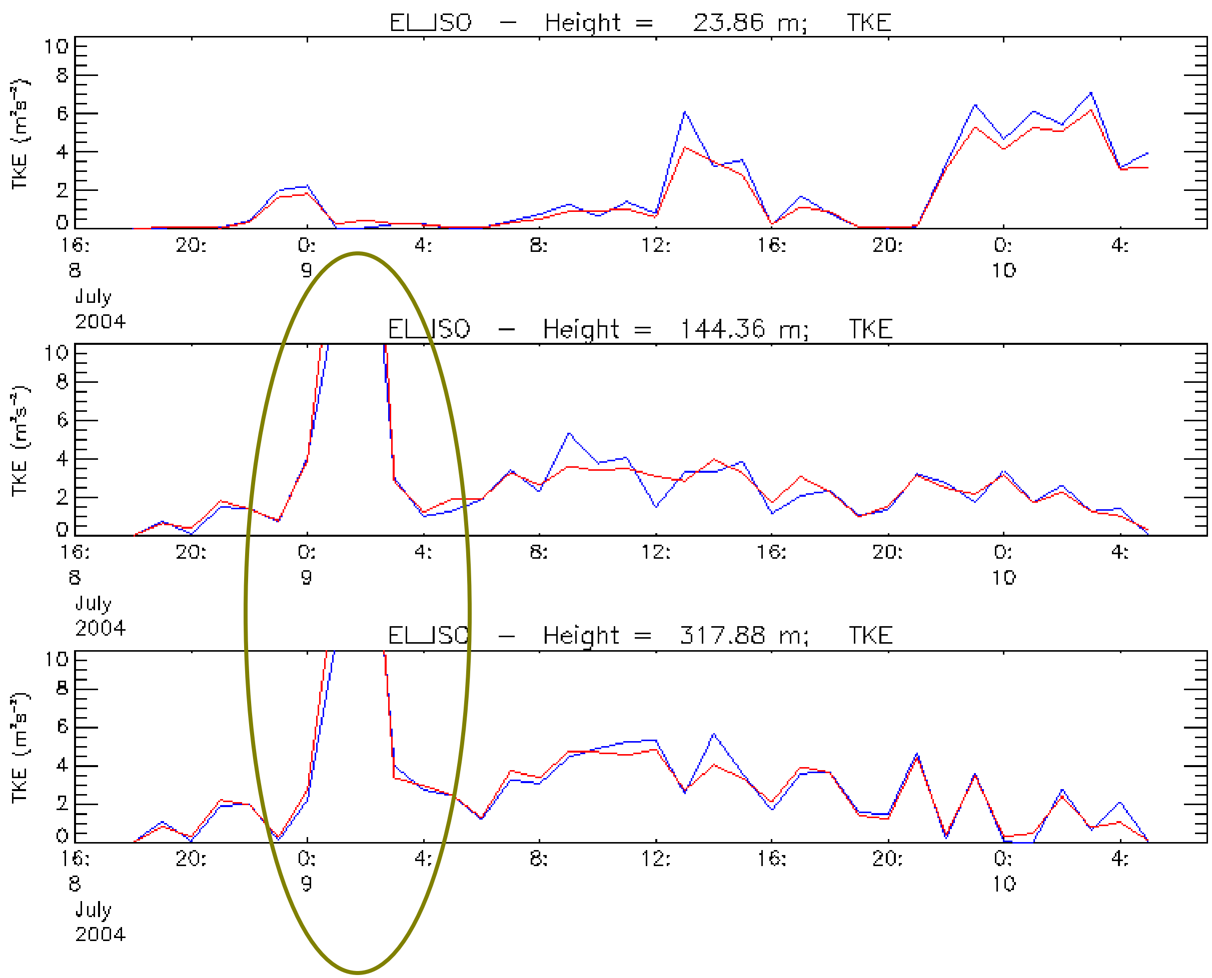

Red: G3_INTP TKE values
Blue: G4 TKE values

Time trend of TKE for G3_INTP and G4 values at three model levels EL_anis scheme

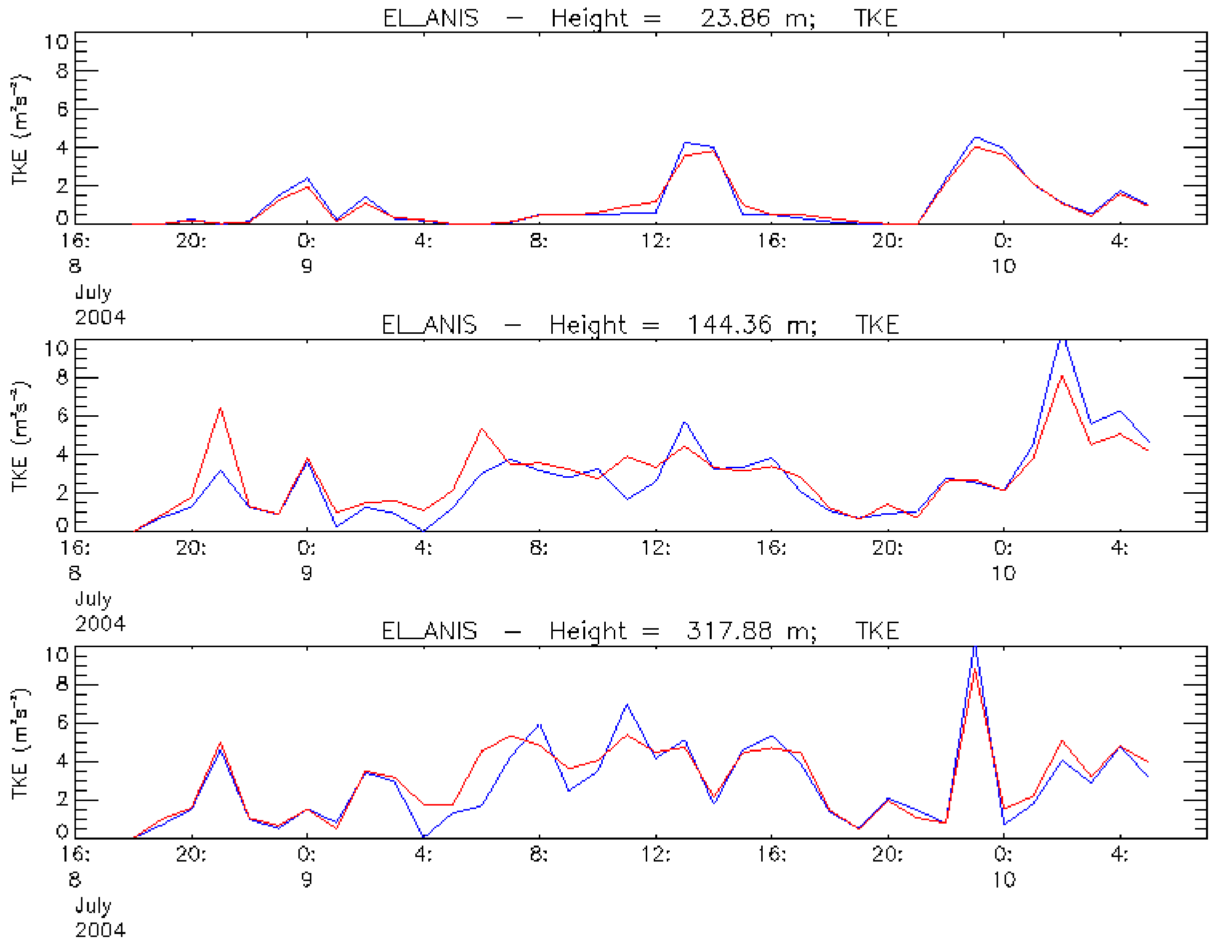

Red: G3_INTP TKE values

Blue: G4 TKE values

Distributions of TKE ratio between G3_INTP and G4 values (TKE < 10 m^2s^{-2})

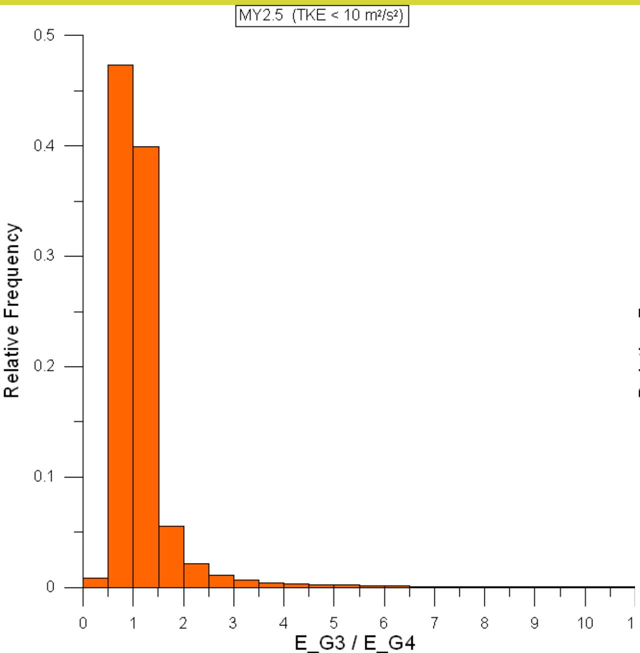

MY2.5

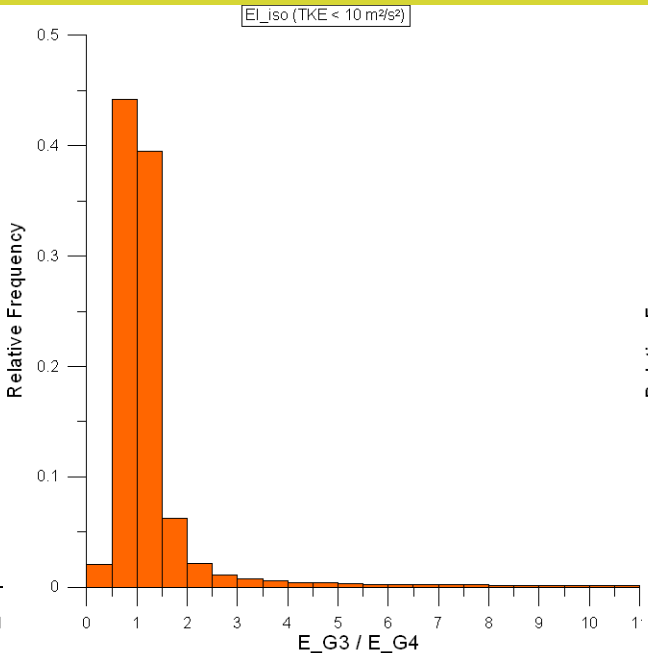

EL_iso

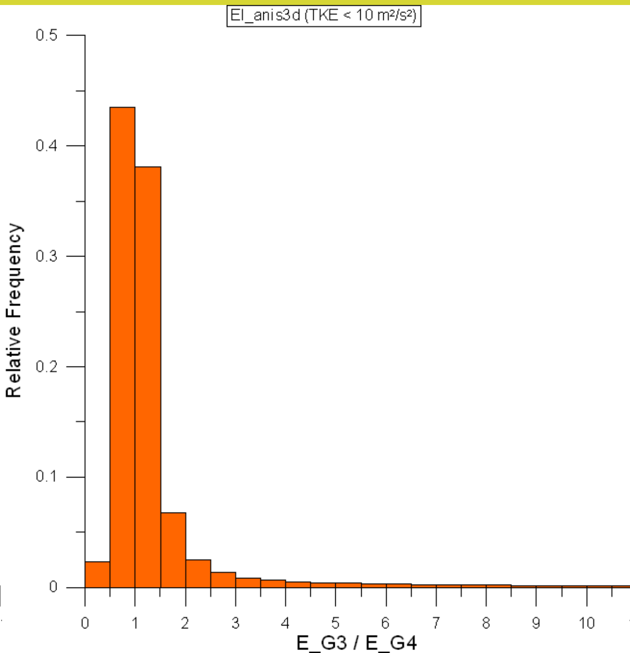

EL_anis

Turbulence intensity

10 GMT

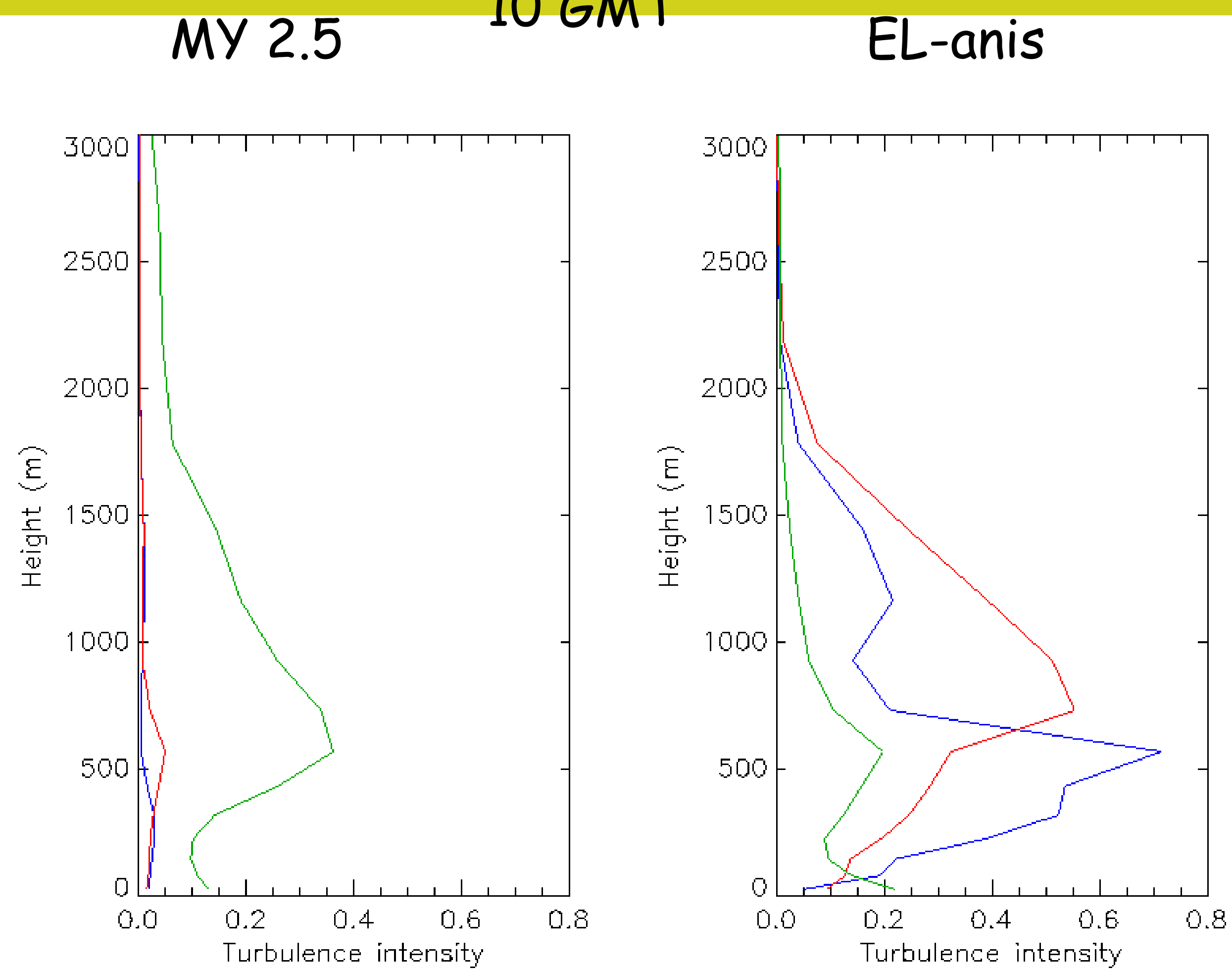

Red: RAMS G3_INTP
Blue: RAMS G4
Green: (RAMS G3 mean flow →) MINERVE+ Hanna

A critical case in complex terrain, 15 GMT (MY closure)

RAMS closure scheme	Friction velocity u_* (ms^{-1})	Temperature scale θ_* (K)	Monin-Obukhov length L (m)	PBL height h (m)
MY2.5	0.38	1.52	-46.01	1174.
E/-anis	0.37	1.54	-41.85	1298.

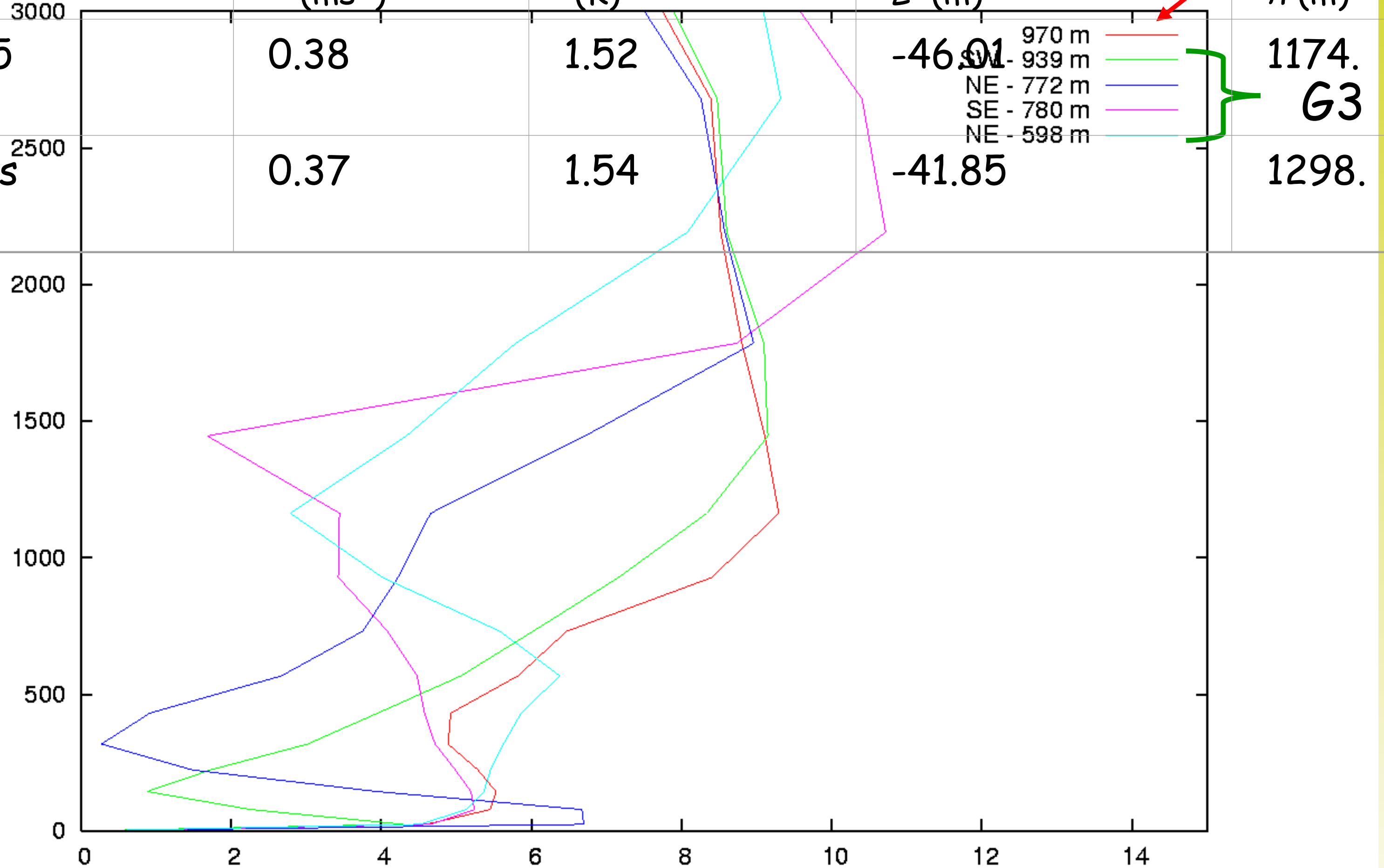

A critical case in complex terrain, speed

15 GMT

MY 2.5 EL-anis

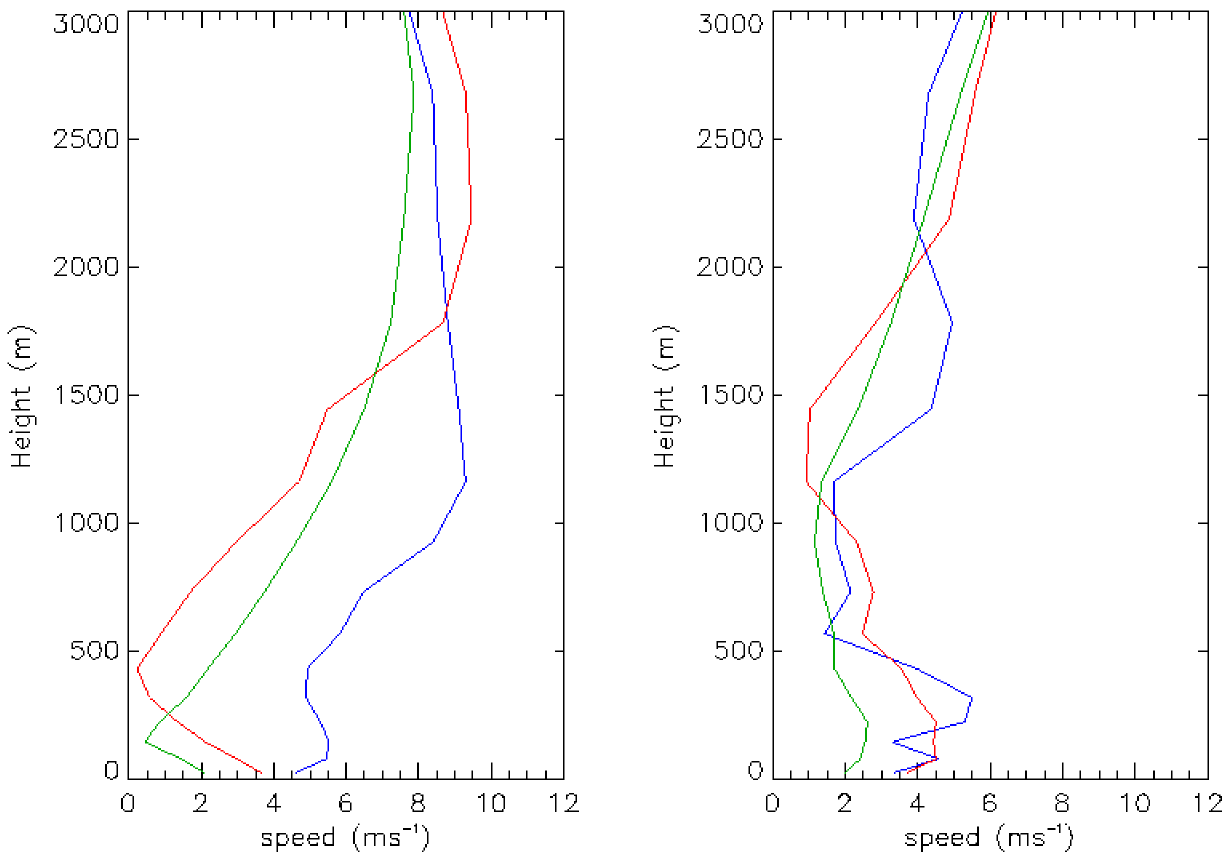

Red: RAMS G3_intp
Blue: RAMS G4
Green: (RAMS G3 mean flow →) MINERVE

A critical case in complex terrain, TKE

15 GMT

MY 2.5 | EL-anis

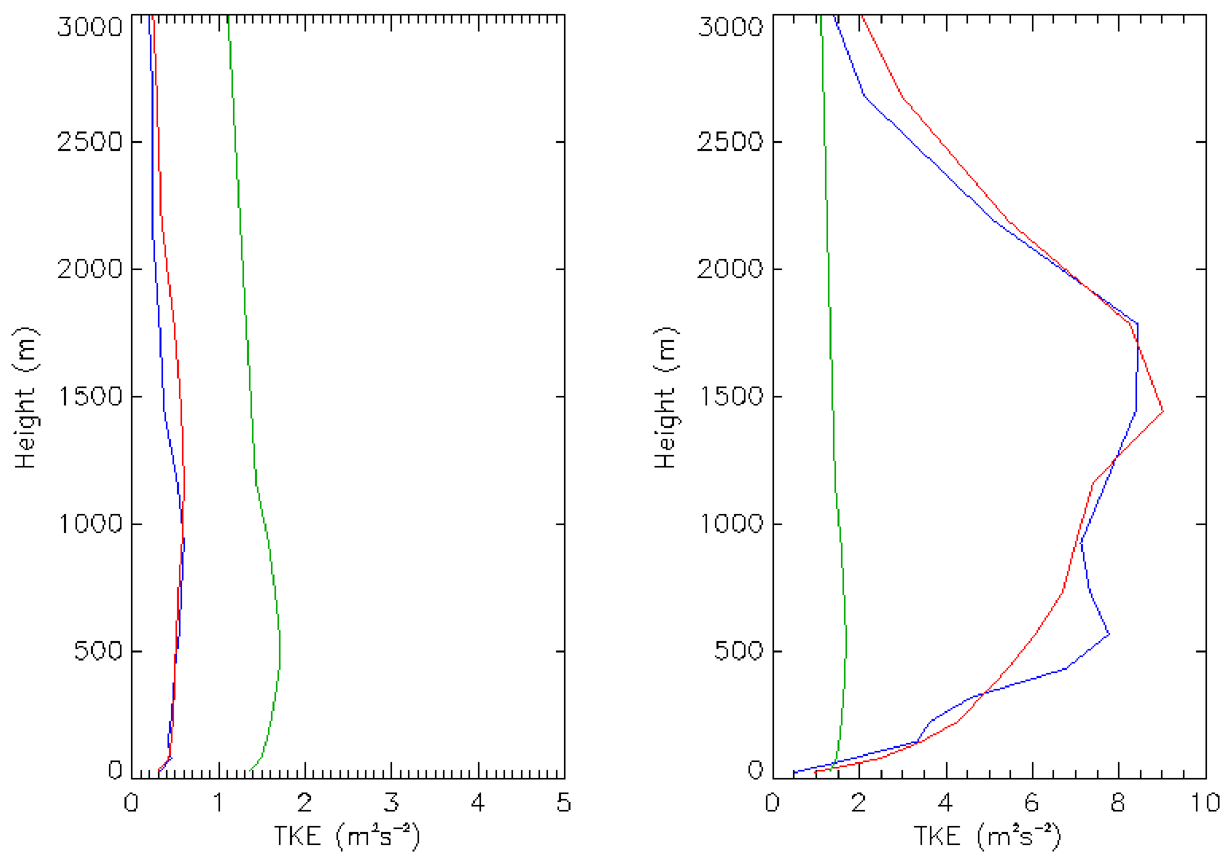

Red: RAMS G3_intp

Blue: RAMS G4

Green: (RAMS G3 mean flow →) MINERVE+Hanna

Conclusions on preliminary analisys

Interpolated values of TKE from 1 km resolution grid (G3_INTP) result to be overall representative of the TKE values simulated on a 250 m grid (G4).

The spread between the two sets of TKE values, G3_INTP and G4 are probably mainly due to the fact that the G3 points, on which the interpolation procedure is applied, may be characterized by even significantly different altitudes

Unlikely high TKE values are produced for EL_type closures:
- at the boundaries of the domains
- at the nesting boundary
- in correspondence with changing orography

probably due to discontinuities in the flow inducing high velocity gradients, therefore high turbulence production.
- also at heights over the boundary layer and during the night

probably generated by numerical instabilities when the turbulence quantities assume low threshold values.

The methodology seems to be feasible, also in complex terrain and in critical locations. A quantitative analysis versus observed data and further investigations, also on the subsequent effects on the dispersion modelling, are under process